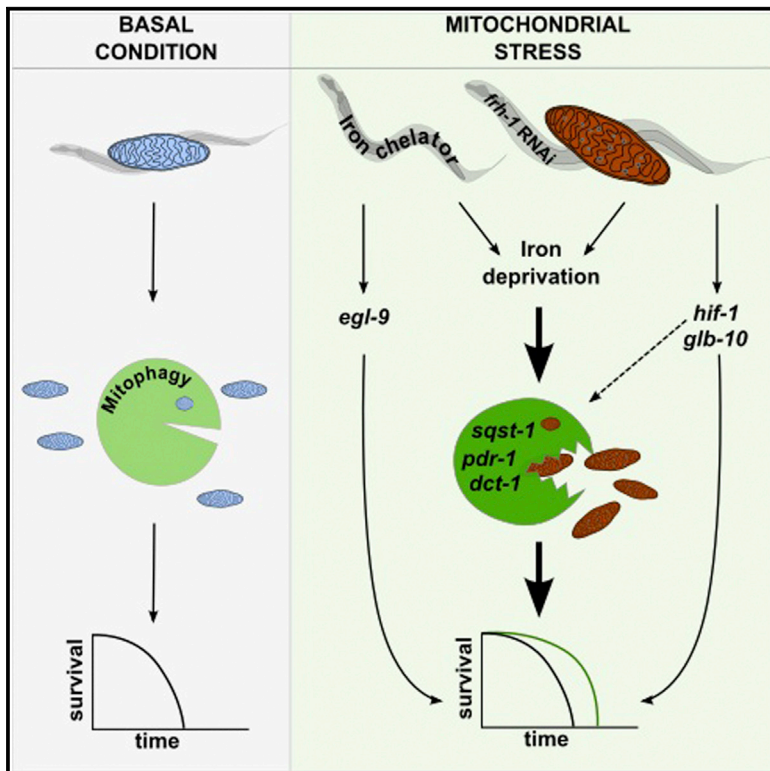


## Iron-Starvation-Induced Mitophagy Mediates Lifespan Extension upon Mitochondrial Stress in *C. elegans*

### Graphical Abstract



### Authors

Alfonso Schiavi, Silvia Maglioni, Konstantinos Palikaras, ..., Francesco Cecconi, Nektarios Tavernarakis, Natascia Ventura

### Correspondence

natascia.ventura@uni-duesseldorf.de

### In Brief

Mitophagy is a fundamental mitochondrial quality control mechanism. Schiavi et al. identify a conserved Parkin/Bnip3-regulated mitophagy pathway required for lifespan extension induced by mitochondrial stress in *C. elegans*. Mitophagy also mediates a pro-longevity iron starvation response activated to cope with frataxin suppression.

### Highlights

- Mitochondrial stress induces Parkin/Bnip3-regulated mitophagy in *C. elegans*
- Frataxin silencing triggers a pro-longevity iron starvation response
- Mitochondrial stress and iron depletion extend *C. elegans* lifespan via mitophagy
- Frataxin and iron depletion extend lifespan via overlapping and unique mechanisms



# Iron-Starvation-Induced Mitophagy Mediates Lifespan Extension upon Mitochondrial Stress in *C. elegans*

Alfonso Schiavi,<sup>2,3</sup> Silvia Maglioni,<sup>1,2</sup> Konstantinos Palikaras,<sup>4</sup> Anjumara Shaik,<sup>1,2</sup> Flavie Strappazon,<sup>6,7</sup> Vanessa Brinkmann,<sup>2</sup> Alessandro Torgovnick,<sup>2</sup> Natascha Castelein,<sup>9</sup> Sasha De Henau,<sup>9</sup> Bart P. Braeckman,<sup>9</sup> Francesco Ceconi,<sup>6,7,8</sup> Nektarios Tavernarakis,<sup>4,5</sup> and Nataschia Ventura<sup>1,2,3,\*</sup>

<sup>1</sup>Institute for Clinical Chemistry and Laboratory Diagnostic, Medical Faculty of the Heinrich Heine University, 40225 Düsseldorf, Germany

<sup>2</sup>IUF-Leibniz Research Institute for Environmental Medicine, 40225 Düsseldorf, Germany

<sup>3</sup>Department of Biomedicine and Prevention, University of Rome Tor Vergata, 00133 Rome, Italy

<sup>4</sup>Institute of Molecular Biology and Biotechnology, Foundation for Research and Technology – Hellas, Heraklion 70013, Crete, Greece

<sup>5</sup>Department of Basic Sciences, Faculty of Medicine, University of Crete, Heraklion 71110, Crete, Greece

<sup>6</sup>IRCCS Fondazione Santa Lucia, 00143 Rome, Italy

<sup>7</sup>Department of Biology, University of Rome Tor Vergata, 00133 Rome, Italy

<sup>8</sup>Unit of Cell Stress and Survival, Danish Cancer Society Research Center, 2100 Copenhagen, Denmark

<sup>9</sup>Biology Department, Ghent University, 9000 Ghent, Belgium

\*Correspondence: [nataschia.ventura@uni-duesseldorf.de](mailto:nataschia.ventura@uni-duesseldorf.de)

<http://dx.doi.org/10.1016/j.cub.2015.05.059>

## SUMMARY

Frataxin is a nuclear-encoded mitochondrial protein involved in the biogenesis of Fe-S-cluster-containing proteins and consequently in the functionality of the mitochondrial respiratory chain. Similar to other proteins that regulate mitochondrial respiration, severe frataxin deficiency leads to pathology in humans—Friedreich’s ataxia, a life-threatening neurodegenerative disorder—and to developmental arrest in the nematode *C. elegans*. Interestingly, partial frataxin depletion extends *C. elegans* lifespan, and a similar anti-aging effect is prompted by reduced expression of other mitochondrial regulatory proteins from yeast to mammals. The beneficial adaptive responses to mild mitochondrial stress are still largely unknown and, if characterized, may suggest novel potential targets for the treatment of human mitochondria-associated, age-related disorders. Here we identify mitochondrial autophagy as an evolutionarily conserved response to frataxin silencing, and show for the first time that, similar to mammals, mitophagy is activated in *C. elegans* in response to mitochondrial stress in a *pdr-1/Parkin*-, *pink-1/Pink*-, and *dct-1/BNIP3*-dependent manner. The induction of mitophagy is part of a hypoxia-like, iron starvation response triggered upon frataxin depletion and causally involved in animal lifespan extension. We also identify non-overlapping *hif-1* upstream (HIF-1-prolyl-hydroxylase) and downstream (globins) regulatory genes mediating lifespan extension upon frataxin and iron depletion. Our findings indicate that mitophagy induction is part of an adaptive iron starvation response induced as a protective mechanism against mitochondrial stress,

thus suggesting novel potential therapeutic strategies for the treatment of mitochondrial-associated, age-related disorders.

## INTRODUCTION

Frataxin is a nuclear-encoded mitochondrial protein that regulates the biogenesis of iron-sulfur-cluster (ISC)-containing proteins and, as a consequence, the functionality of the mitochondrial respiratory chain (MRC). Complete absence of frataxin is lethal in different species, including the nematode *Caenorhabditis elegans* (*C. elegans*), and its severe deficiency leads in humans to Friedreich’s ataxia (FRDA), the most frequently inherited recessive ataxia [1]. Similar to other life-threatening mitochondrial-associated diseases, residual levels of the pathogenic protein (frataxin) is critical for survival and inversely correlates with disease onset, progression, and severity of symptoms. According to a threshold effect, moderate depletion of the *C. elegans* frataxin homolog FRH-1, similar to suppression of other mitochondrial-associated diseases proteins, extends animal lifespan [2]. The evolutionarily conserved nature of this pro-longevity effect [3] indicates that cellular adaptation to partial mitochondrial dysfunction induces beneficial responses, which, if identified, may suggest novel therapeutic strategies for human diseases associated with progressive mitochondrial deterioration [4].

Changes in animal metabolism and induction of cellular stress responses and detoxification systems (e.g., mtUPR, antioxidants, and autophagy) have been associated with, although not always causally involved in, lifespan extension in animals with genetic- or RNAi-mediated suppression of MRC regulatory proteins (the so-called mitochondrial [*Mit*] mutants [4, 5]). However, the key molecular players underlying mitochondrial-stress control of longevity are still largely uncharacterized. To date, only some autophagy (*unc-51* and *bec-1*) and mtUPR (*ubl-5*) regulatory genes [6, 7], as well as a handful of transcription factors [5] (the *C. elegans* p53 ortholog CEP-1, the homeobox protein CEH-23,

a component of the TFIID mRNA transcription complex TAF-4, the *C. elegans* TFEB ortholog HLH-30, and the hypoxia-inducible factor HIF-1), were shown to mediate *Mit* mutants longevity.

HIF-1 overexpression or stabilization through hypoxia or reduced expression of *egl-9* or *vhl-1* extends *C. elegans* lifespan [8, 9]. EGL-9 is the prolyl-hydroxylase that in normoxia conditions targets HIF-1 to the proteasome for degradation through VHL-1, the von Hippel Lindau protein that is part of an E3 ubiquitin-ligase complex. The activity of EGL-9 is inhibited by low oxygen levels but also by reduced levels of iron and of the tricarboxylic cycle acid intermediate ( $\alpha$ KG) [10]. Induction of autophagy is an evolutionarily conserved protective response to hypoxia and to reduced frataxin expression, and it is required for mitochondrial-stress extension of lifespan in *C. elegans* [6, 11]. Mitochondrial autophagy (or mitophagy) is a selective form of autophagy dedicated to mitochondrial quality control by recycling unhealthy mitochondria [12]. It can be activated in a HIF-1- and Beclin-dependent manner to protect mammalian cells against hypoxia [13]. Whether mitophagy plays a role in mitochondrial-stress control of longevity remains speculative [14, 15] and was the main question addressed in this study.

Here we provide evidence that in *C. elegans* a hypoxia-like iron starvation response is causally involved in the lifespan-extending effect elicited by frataxin suppression, and we identify mitochondrial autophagy as part of this beneficial response. We find that mitophagy is induced in an evolutionarily conserved manner upon frataxin silencing, and we show for the first time that, similar to mammals, it is activated in *C. elegans* in response to mitochondrial stress in a Parkin/*pdr-1*-, Pink/*pdr-1*-, and Bnip3/*dct-1*-dependent manner. Furthermore, although different mitophagy regulatory homologs mediate *C. elegans* lifespan extension upon frataxin or iron depletion, we find that the two treatments can extend lifespan also through unique, non-overlapping mechanisms. We, therefore, provide further insight into molecular mechanisms of mitochondrial-stress control of longevity and point to mitophagy as a novel potential therapeutic target for FRDA and possibly other mitochondrial-associated diseases.

## RESULTS

### *C. elegans* Homologs of Mitophagy Regulatory Genes Mediate Lifespan Extension

Induction of autophagy is an evolutionarily conserved response to reduced frataxin expression, causally involved in the longevity of different *C. elegans Mit* mutants including frataxin (*frh-1*)-depleted animals [6]. Mitochondrial autophagy is a selective form of autophagy dedicated to mitochondrial quality control, which is activated to recycle unhealthy mitochondria. We thus asked whether mitophagy could play a specific role in mitochondrial-stress control of longevity. In mammals, Pink1 kinase cooperates with Parkin, a cytosolic E3 ubiquitin ligase, to signal damaged mitochondria for degradation through autophagy [16]. Homologs of the genes that encode for these proteins have been identified in *C. elegans*, respectively named *pink-1* and *pdr-1*, and their deletion increases animal's sensitivity to oxidative stress [17, 18]. Silencing of *pink-1* was also recently shown to prevent proper elimination of damaged mtDNA after UVC irradiation [19]. To address the role of *pink-1* and *pdr-1* in longevity specification in response to mitochondrial stress, we assessed

the lifespan of corresponding mutant strains upon frataxin silencing. We found that the lifespan-extending effect of *frh-1* RNAi was almost completely prevented in the *pdr-1(gk448)* mutant strain (Figures 1A and 1B; Table S1). Two additional *pdr-1* alleles (*tm598* and *tm395*), as well as *pdr-1* RNAi, also suppressed the lifespan-extending ability of frataxin silencing (Figures S1A–S1C; Table S1), thus establishing a clear role for *pdr-1* in frataxin-regulated longevity. To our surprise, but consistent with recent finding from Bess et al. [19] showing seemingly contrasting results between *pink-1* mutant and silencing, two different *pink-1* mutant alleles (*tm1779* and *ok3538*) did not affect *frh-1* RNAi longevity, while *pink-1* RNAi completely abolished it (Figures S1D–S1F; Table S1).

We then tested the effect of other possible mitophagy regulatory genes, such as Bnip3 (*dct-1* in *C. elegans* [20]), the Bcl-2/adenovirus E1B 19-kDa-interacting protein 3, and the adaptor protein p62/SQST1 (*sqst-1* in *C. elegans* [21]). We found that deletion or silencing of *C. elegans dct-1* suppressed *frh-1* RNAi extension of lifespan compared to its effect on the wild-type strain (Figures 1C and S1G; Table S1). Moreover, *C. elegans sqst-1* mutants completely abolished the lifespan-extending effect of *frh-1* RNAi (Figure 1D). In mammals, Bnip3 is induced to eliminate dysfunctional mitochondria in response to hypoxia in an HIF-1-dependent manner [13], while p62 facilitates cargo degradation, including mitochondria, and it is selectively degraded in response to hypoxia through the autophagic machinery [22]. Likewise, we now found that in *C. elegans* hypoxia upregulates the expression of *dct-1* in an *hif-1*-dependent manner (Figures S1H and S1I). Moreover, hypoxia reduced the content of the SQST-1 protein in a wild-type background and upon loss of the ribosomal protein *rpl-43*, which has been shown to cause an accumulation of SQST-1 aggregates [23] (Figures S1J and S1K). Of note, similar to a hypoxia mechanism, frataxin silencing increased the expression of *dct-1* transcript in an *hif-1*-dependent manner and reduced that of SQST-1 protein (Figures 1E and 1F). We did not observe any change in p62 transcript expression upon *frh-1* RNAi (data not shown), indicating that its degradation occurs at the posttranscriptional level, possibly through an intact autophagic flux [6] induced by a hypoxia-like signaling. Taken together, these findings revealed an evolutionarily conserved protective role for mitophagy regulatory genes, which are required for frataxin-silencing extension of lifespan in *C. elegans*.

### Induction of Mitophagy Is an Evolutionarily Conserved Response to Mitochondrial Stress

The inability of *frh-1* RNAi to extend lifespan in mutants of mitophagy regulatory homologs could be ascribed to mitophagy-independent functions of the corresponding *C. elegans* proteins. Indeed, whether *C. elegans* mitophagy is induced upon mitochondrial stress and regulated by the same genes is not known. We, therefore, assessed whether *frh-1* silencing affects mitophagy. Compared to control animals, *frh-1* RNAi-treated animals displayed a substantial co-localization between mitochondria and autophagosomal marker LGG-1 (Figures 2A and S2A), a prerequisite for mitochondrial elimination through the autophagic pathway. To further prove the induction of mitochondrial autophagy, we generated additional transgenic strains and found that frataxin silencing significantly increased the co-localization between DCT-1 and LGG-1 and between DCT-1 and PDR-1

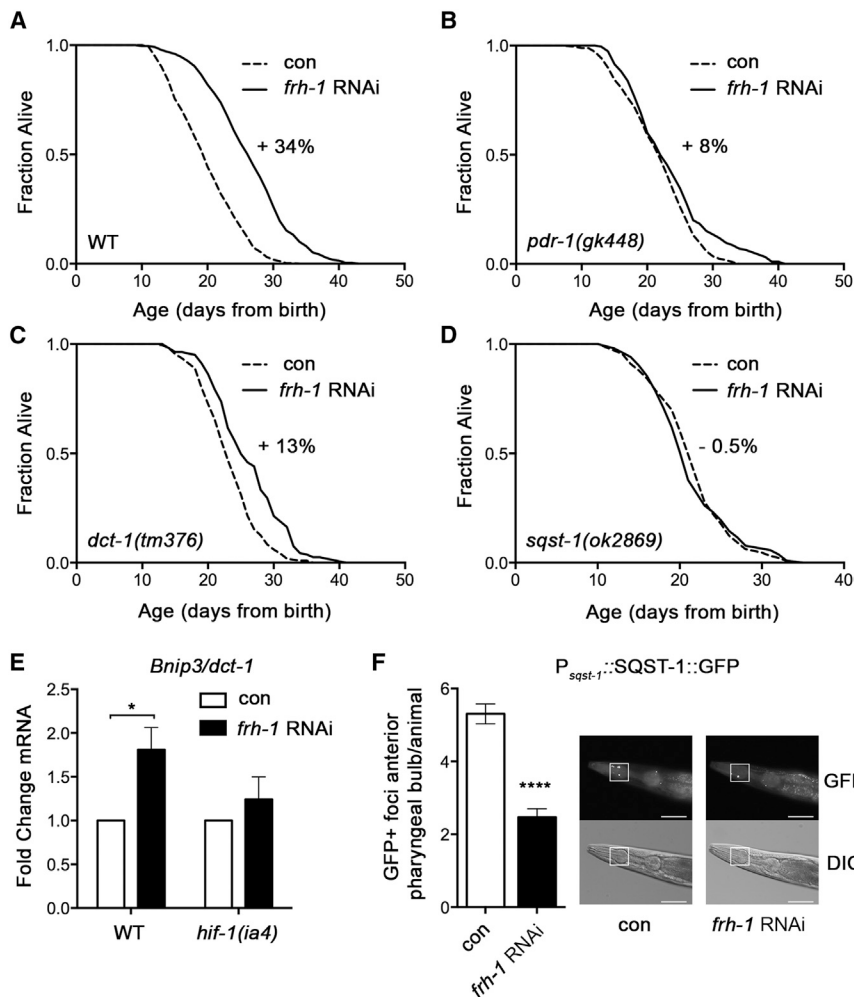


### Figure 1. *C. elegans* Homologs of Mitophagy Regulatory Genes Mediate Lifespan Extension upon Frataxin Silencing

(A–D) Kaplan-Meier survival curves of wild-type (WT) (A), *pdr-1(gk448)* (B), *dct-1(tm376)* (C), and *sqst-1(ok2869)* (D) *C. elegans* strains fed bacteria transformed with either empty-vector (con) or vector-expressing dsRNA against *frh-1* (*frh-1* RNAi). Percentages indicate increase in mean lifespan of *frh-1* RNAi-treated over control animals. (E) Quantification of *dct-1* transcript expression in WT animals and *hif-1* mutants fed as in (A). Bar graph represents means  $\pm$  SEM (n = 3); \*p < 0.05. (F) Quantification of GFP+ foci in the anterior pharyngeal bulb of *P<sub>sqst-1</sub>::SQST-1::GFP* transgenic strain fed as in (A). (Right) Representative pictures have red squares indicating the region used to count the number of foci. (Top) Green fluorescence channel images (GFP) are shown. (Bottom) Differential (Nomarski) interference contrast images (DICs) are shown. Scale bars in white represent 50  $\mu$ m. Bar graph represents means  $\pm$  SEM (n = 5); \*\*\*\*p < 0.0001. See also Figures S1 and S3.

compared to wild-type animals (Figures S2B and S2C). Collectively, these data clearly demonstrate that *frh-1*-depleted animals display an increased number of mitoautophagosomes compared to wild-type animals.

To confirm the induction of mitochondrial autophagy in *C. elegans*, we expressed a dual fluorescent pH-sensitive biosensor with a mitochondrial tag that, in normal conditions, marks mitochondria in red and green fluorescence. Upon mitophagy induction, the delivery of mitochondria into the acidic lysosome compartment mainly quenches the green, but not the red, fluorescence, thus reducing the GFP to dsRed ratio (see the Supplemental Experimental Procedures). We observed that *frh-1* RNAi significantly reduced the ratio of GFP versus dsRed fluorescence (Figures 2B and 2C), a clear indication of mitochondria redistribution into the lysosomal compartment. Of note, silencing of mitophagy regulatory genes required for frataxin longevity significantly prevented the induction of mitochondrial autophagy upon *frh-1* RNAi without affecting it in basal conditions (Figure 2C), indicating that mitophagy is required for lifespan extension upon mitochondrial stress.

Remarkably, considering the potential role of mitophagy in the context of neurodegenerative diseases [15], we also found that mitochondrial autophagy is triggered by frataxin silencing in

mammalian cells. In agreement with our previous findings [6], compared to control cells, frataxin small hairpin RNA (shRNA)-treated cells expressed increased levels of LC3II (Figure 2D). Consistent with an increased mitochondrial autophagy, frataxin-depleted cells also contained fewer mitochondrial proteins, such as MnSOD and TOM20 (Figure 2D). Moreover, confocal microscopic analysis revealed Parkin translocation from the cytosol to the mitochondria (Figure S2D), a signal

required for targeting mitochondria to the autophagic machinery [16]. Cellular fractionation analysis confirmed a significant increase in Parkin as well as Pink accumulation on mitochondria (Figures 2E, 2F, S2E, and S2F). Notably, similar to what we observed in the worms, the expression of p62/SQSTM1, which cooperates with Parkin to facilitate mitochondrial degradation through the lysosomes [24], was reduced in total extracts and mitochondrial-enriched fractions of frataxin shRNA mammalian cells (Figures 2D and S2F), indicating an intact autophagic flux. To maintain an appropriate mitochondrial network homeostasis, induction of mitophagy typically is preceded by mitochondrial fragmentation [25], which favors the elimination of dysfunctional mitochondria, and is accompanied by the biogenesis of new healthy mitochondria. We observed an altered mitochondrial distribution in both mammalian cells and *C. elegans* subjected to frataxin silencing, an indication of an effective integration of mitochondrial quality control pathways. Indeed, confocal analysis of frataxin shRNA-treated cells revealed a clear perinuclear clustering of highly fragmented mitochondria (Figure S2D), a typical distribution of mitochondria undergoing mitophagy [24]. Similarly, *frh-1* silencing in *C. elegans* increased the density of muscle mitochondria, which also presented with a fragmented pattern (Figure S2G).



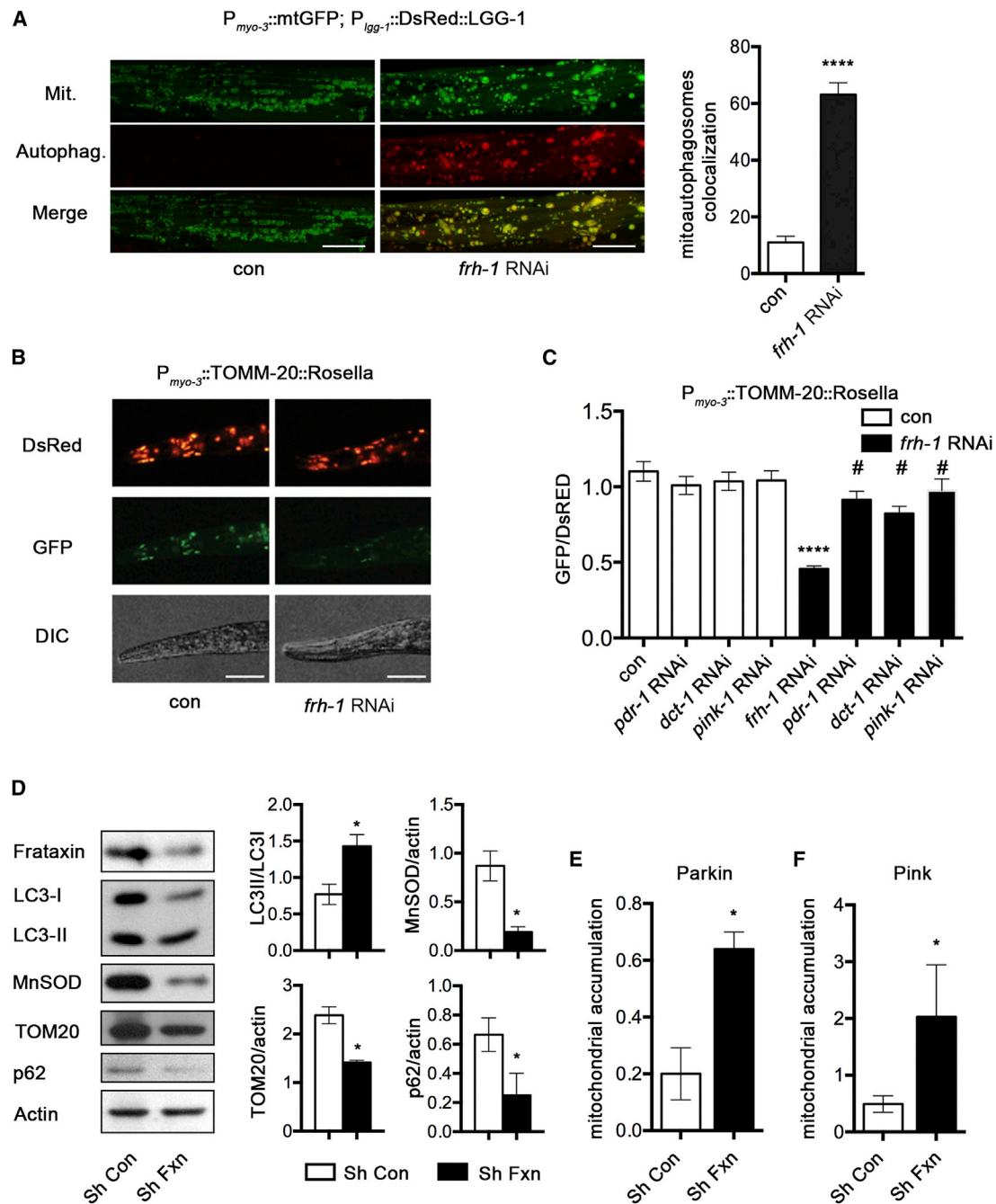


### Figure 2. Induction of Mitophagy Is an Evolutionarily Conserved Response to Frataxin Silencing

(A) Quantification of the colocalization between mitochondria and autophagosomes in  $P_{myo-3}::mtGFP; P_{lgg-1}::DsRed::LGG-1$  transgenic animals fed bacteria transformed with either empty-vector (con) or vector-expressing dsRNA against *frh-1* (*frh-1* RNAi). (Left) Representative confocal picture of *C. elegans* muscles was acquired using a 100 $\times$  objective lens; green, muscle mitochondria (Mit); red, autophagosomes (Autophag.); and yellow, overlapping of the two (Merge). Size bars, 20  $\mu$ m. (B) Representative pictures show  $P_{myo-3}::TOMM-20::Rosella$  transgenic strain fed as in (A). In red is shown the total amount of mitochondria as revealed by pH-insensitive Rosella red tag (dsRED), and in green is shown the amount of mitochondria that is transported to the lysosome as revealed by pH-sensitive Rosella green tag (GFP). (Bottom) DIC shows the part of the animals used for quantification.

(C) Mitochondrial autophagy was quantified using the ratio between green and red fluorescence (GFP/DsRED) in  $P_{myo-3}::TOMM-20::Rosella$  transgenic animals fed bacteria transformed with either empty vector (con) or vector expressing the indicated dsRNA.

(D) Representative western blots and quantifications of the expression of the indicated proteins from human embryonic kidney HEK293 cells transiently transfected with vector-expressing shRNA control (Sh Con) or shRNA Frataxin (Sh Fxn) are shown.

(E and F) Quantification of Parkin (E) and Pink (F) accumulation on mitochondria from enriched mitochondrial extract of HEK293 cells treated as in (D).

Bar graphs represent means  $\pm$  SEM ( $n = 3$ ); \*p value versus con < 0.05, \*\*\*\*p value versus con < 0.0001, #p value versus *frh-1* RNAi < 0.0001. See also Figures S2 and S3.

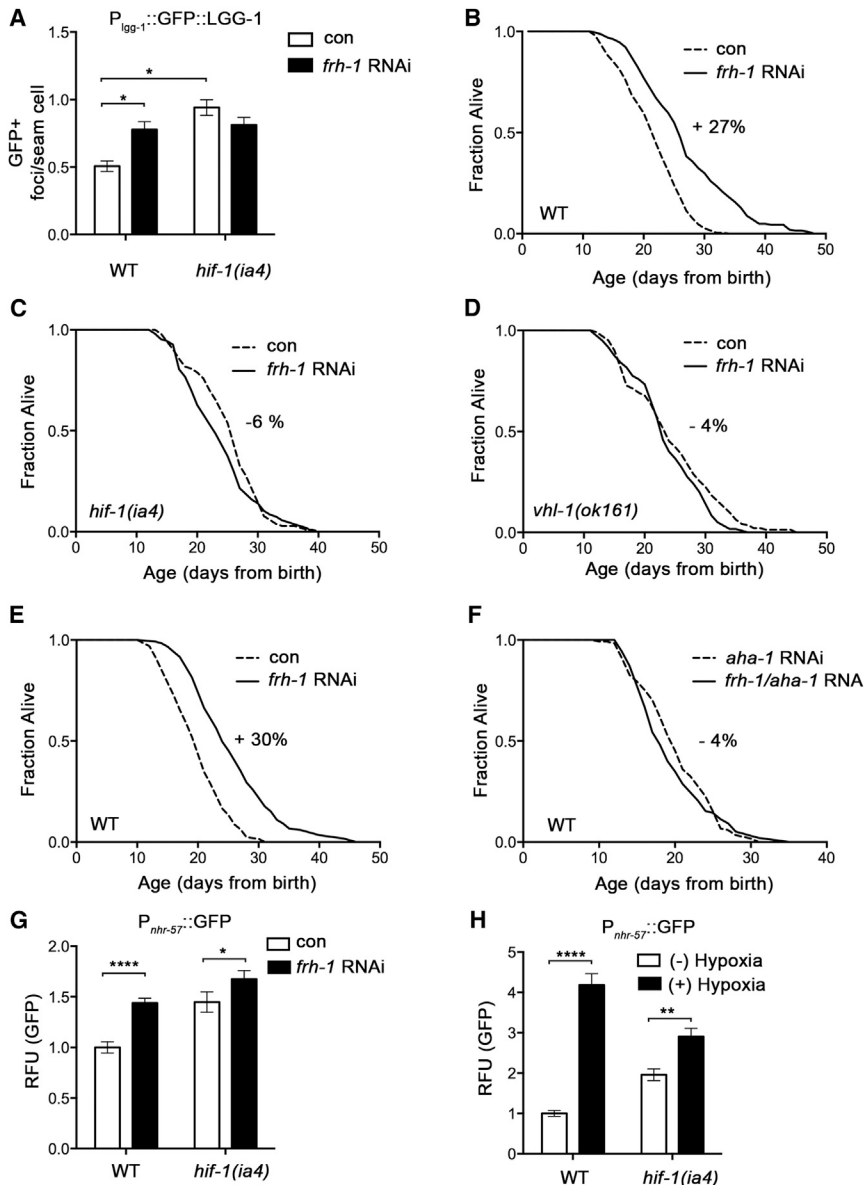


### Figure 3. Frataxin Silencing Induces a Hypoxia-like Signaling

(A) Quantification of GFP<sup>+</sup> foci in the seam cells of  $P_{lgg-1}::GFP::LGG-1$  (WT) and  $P_{lgg-1}::GFP::LGG-1$ ; *hif-1(ia4)* transgenic strains fed bacteria transformed with either empty-vector (con) or vector-expressing dsRNA against *frh-1* (*frh-1* RNAi). Bar graph represents means  $\pm$  SEM (n = 5); \*p < 0.05. (B–D) Kaplan-Meier survival curves of WT (B), *hif-1(ia4)* (C), and *vhl-1(ok161)* (D) *C. elegans* strains fed as in (A) are shown. (E and F) Kaplan-Meier survival curves of WT animals fed bacteria transformed either with empty-vector (con) or with vector-expressing dsRNA against *frh-1* (*frh-1* RNAi), *aha-1* (*aha-1* RNAi), or both (*frh-1/aha-1* RNAi). Percentages indicate increase or decrease in mean lifespan of *frh-1* RNAi-treated over control animals. (G) Quantification of GFP expression in WT and *hif-1(ia4)* strains expressing the  $P_{nhr-57}::GFP$  transgene fed as in (A) is shown. (H) Quantification of GFP expression in WT and *hif-1(ia4)* strains expressing the  $P_{nhr-57}::GFP$  transgene and fed empty vector transformed bacteria were left untreated or treated for 4 hr with hypoxia (<1% O<sub>2</sub> at 20°C). Bar graph represents means  $\pm$  SEM (n = 3); \*p value vs con < 0.05, \*\*\*\*p value versus con < 0.0001. See also Figure S4.

Finally, in support of a general conserved role for mitophagy in response to mitochondrial stress, we found that silencing other MRC regulatory proteins, similar to *frh-1* RNAi [6], reduced reactive oxygen species (ROS) levels (Figure S3A); increased the accumulation of autophagosomes (Figure S3B); promoted a *pdr-1*-, *dct-1*-, and *pink-1*-dependent mitophagy (Figure S3C); and required mitophagy regulatory genes for optimal lifespan extension (Figures S3D–S3G). Collectively, the results described so far indicate that the induction of mitochondrial autophagy is an evolutionarily conserved response to reduced frataxin expression, and they identify a role for *pdr-1*/Parkin- and *dct-1*/Bnip3-regulated mitophagy in mitochondrial-stress control of longevity.

### Frataxin Silencing Induces a Pro-longevity Iron Starvation Response

In search of a mechanism that could explain how frataxin depletion stimulates mitochondrial autophagy, we speculated a

possible hypoxia-like signal triggered by altered mitochondrial physiology. Indeed, frataxin suppression affects intracellular levels of ATP, ROS, and iron [6, 26], which can initiate a hypoxia-like signaling [27, 28]. Hypoxia, in turn, can trigger autophagy in *C. elegans* [11] as well as in mammals, and in the latter this can occur either in an HIF-1-dependent manner [29] or in an HIF-1-independent manner through AMP-regulated kinases (AMPKs) [30]. Although ATP content is reduced in *frh-1* RNAi-depleted animals and in other RNAi-derived *Mit* mutants, levels of ATP do not correlate with, and AMPKs do not mediate, animal longevity [6, 31], thus arguing against a potential AMPK-regulated, HIF-1-independent activation of autophagy. Instead, *hif-1* is required for lifespan extension in other *Mit* mutants [28, 32], and we found that it mediates autophagy and longevity in *frh-1* RNAi animals (Figures 3A–3C). Specifically, LGG-1 is the nematode homolog of the microtubule-associated protein light chain 3 (LC3), and its pattern changes from diffuse to punctate during the autophagic process, reflecting the formation of the autophagosomes [33]. While *frh-1* RNAi induces the accumulation of LGG-1-positive foci in wild-type animals [6], it could not further increase it in the *hif-1* mutants, which already presented with a significantly higher number of autophagosomes compared to wild-type animals (Figure 3A). Either stabilization of HIF-1, through hypoxia or through reduced expression of VHL-1, or its loss of function can extend *C. elegans* lifespan [8, 9].

Consistent with an intact autophagy flux being required for *frh-1* RNAi longevity [6], we now found that either *hif-1* or *vhl-1* depletion completely blocked lifespan extension in response to frataxin silencing (Figures 3B–3D). The hypoxia-inducible factor acts in a heterodimeric transcription complex, consisting of HIF-1 and AHA-1 in *C. elegans*, encoded by homologs of the mammalian HIF-1-alpha and -beta subunits, respectively [34]. *aha-1* recently was identified as one of the *C. elegans* transcription factors required for lifespan extension in genetic-mediated *Mit* mutants [32]. In line with the *hif-1* findings, *frh-1* RNAi could not extend lifespan in animals depleted of *aha-1* (Figures 3E and 3F; Table S1). In further support of frataxin silencing activating a hypoxia-like response, it increased the expression of hypoxia-inducible genes such as *nhr-57* (Figure 3G) and *dct-1* (Figure 1E) in an *hif-1*-dependent manner, and reduced the expression of p62 (Figure 1F). In *C. elegans*, *nhr-57* belongs to the large family of nuclear hormone receptors and it is the most reliable marker for HIF-1 activation under hypoxic conditions ([35] and Figure 3H). Moreover, we found that *frh-1* RNAi tends to increase the transcriptional expression of different globins, *glb-1*, *glb-10*, *glb-13*, *glb-19*, and *glb-28*, especially in an RNAi-sensitized background; but, a *frh-1* double-stranded RNA (dsRNA) construct that reduced frataxin expression above the threshold for lifespan extension [6] did not significantly modulate the expression of any of them (Figures S4A and S4B). Globin genes encode for iron-containing proteins that can regulate the redox status of the cells in response to hypoxia [36]. Thirty-three globins were identified in *C. elegans*, all containing HIF-1 regulatory elements, and some of them can be induced by hypoxia in an *hif-1*-dependent manner ([37] and Figure S4C).

We then asked how frataxin silencing could mimic a hypoxia-like state. HIF-1 is a central player of oxygen and iron homeostasis in mammals as well as in *C. elegans* and can be activated by increased levels of ROS or reduced levels of cytosolic oxygen or iron [27, 38]. Although ROS-dependent activation of HIF-1 mediates longevity of the genetic-derived *Mit* mutants [28], ROS levels were actually reduced following silencing of different MRC regulatory subunits, including *frh-1* (Figure S3A) [6]. Iron deprivation can also activate a hypoxia-like signaling in mammals as well as in *C. elegans* [26, 27], and, accordingly, it increased the expression of *nhr-57* in an *hif-1*-dependent manner (Figure 4A), similar to the above-described effect with *frh-1* RNAi or hypoxia (Figures 3G and 3H). We thus speculated that *frh-1* RNAi activates the hypoxia-like response through cytosolic iron deprivation, a condition associated with reduced frataxin expression from yeast to mammals as a consequence of progressive mitochondrial iron accumulation [26, 39]. Consistent with this possibility, we found that the expression of the *C. elegans* cytosolic aconitase (*aco-1*), which is downregulated in response to iron overload like its mammalian homolog iron regulatory protein-1 (IRP1) [40], was significantly increased in *frh-1*-depleted animals compared to wild-type (Figure 4B). The mitochondrial Fe/S-cluster protein aconitase (*aco-2*) was also upregulated by *frh-1* RNAi (Figure 4B). These effects on the two aconitases possibly represent compensatory responses to the reduced cytosolic iron content and Fe/S-cluster biogenesis induced by frataxin deficiency [26]. The two aconitases also tended to be induced by hypoxia in an *hif-1*-dependent manner (Figures S4D and S4E).

A reduced iron content upon frataxin suppression is expected to decrease animal sensitivity to iron supplementation while increasing their sensitivity to iron deprivation. Accordingly, although iron supplementation through the entire life significantly shortened lifespan [41] of control (–18%) and of *frh-1*-depleted (–8%) animals, the latter were much less affected, as clearly underlined by the differences in their mean lifespan (Figure 4C; Table S1). Frataxin-deficient animals were also more sensitive to the detrimental effects induced by severe iron deprivation on development (Figure 4D), fertility, and fecundity (Figure 4E; Figure S4F). Furthermore, electron microscopic analysis revealed an elevated number of electron-dense granules, indicative of iron deposits [42], in mitochondria, but not in the cytosol, of *frh-1*-depleted animals, which was not observed in wild-type animals (Figure S4G). Of note, these electron-dense granules were detected in mitochondria of tissues, such as the intestine and the muscle, where we also observed the induction of autophagy (Figures S4H and 1F) and mitophagy (Figures 2A–2C).

Remarkably, similar to the opposite effects on lifespan induced by different levels of mitochondrial stress, while severe iron deficiency was lethal (Figure 4D), we found that milder iron deprivation significantly extended lifespan in wild-type animals (Figure 4F; Table S1). In support of frataxin silencing acting through an iron starvation response, iron chelation did not significantly extend lifespan of *frh-1*-depleted animals (Figure 4F; Table S1), while iron supplementation suppressed it (Figure 4C). Moreover, DMT1 is a divalent metal transporter whose expression is induced in mammals to increase intestinal iron transport in conditions of iron deficiency, and a *C. elegans* mutant for the DMT1 homolog, *smf-3*, displays low levels of iron compared to wild-type [38]. In agreement with previous results, we found that *smf-3* mutants have an extended lifespan that is not further prolonged by *frh-1* RNAi (Figures 4I and 4J; Table S1). To validate the iron starvation response induced in frataxin-depleted animals, we quantified the expression of the *C. elegans* ferritin homolog, *ftn-2*, an iron storage protein whose expression is induced in the presence of excessive iron and reduced in response to iron deprivation in an *hif-1*-dependent manner [38]. As expected, the expression of a *ftn-2::gfp* reporter was significantly reduced by iron depletion (Figure 4G). Of note we observed that *frh-1* RNAi also reduced *ftn-2* expression, and, consistent with the survival analysis, the combined treatment with iron depletion did not additively affect the expression of the two *hif-1* target genes, *ftn-2* and *nhr-57* (Figures 4G and 4H). Non-additive effects on *ftn-2* and *nhr-57* expression were similarly observed following iron chelation treatment in animals depleted of other MRC regulatory proteins (unpublished data), suggesting a more general iron starvation response upon mitochondrial stress. Taken together, the results shown so far reveal an iron starvation response as an evolutionarily conserved response to frataxin depletion, with pro-longevity effects in *C. elegans*.

### Frataxin and Iron Depletion Extend Lifespan through Overlapping and Independent Mechanisms

Finally, we asked whether frataxin-silencing extension of lifespan via iron depletion could be ascribed to the induction of mitochondrial autophagy. Consistent with this possibility, we found that a lifespan-extending dose of iron chelation significantly induced

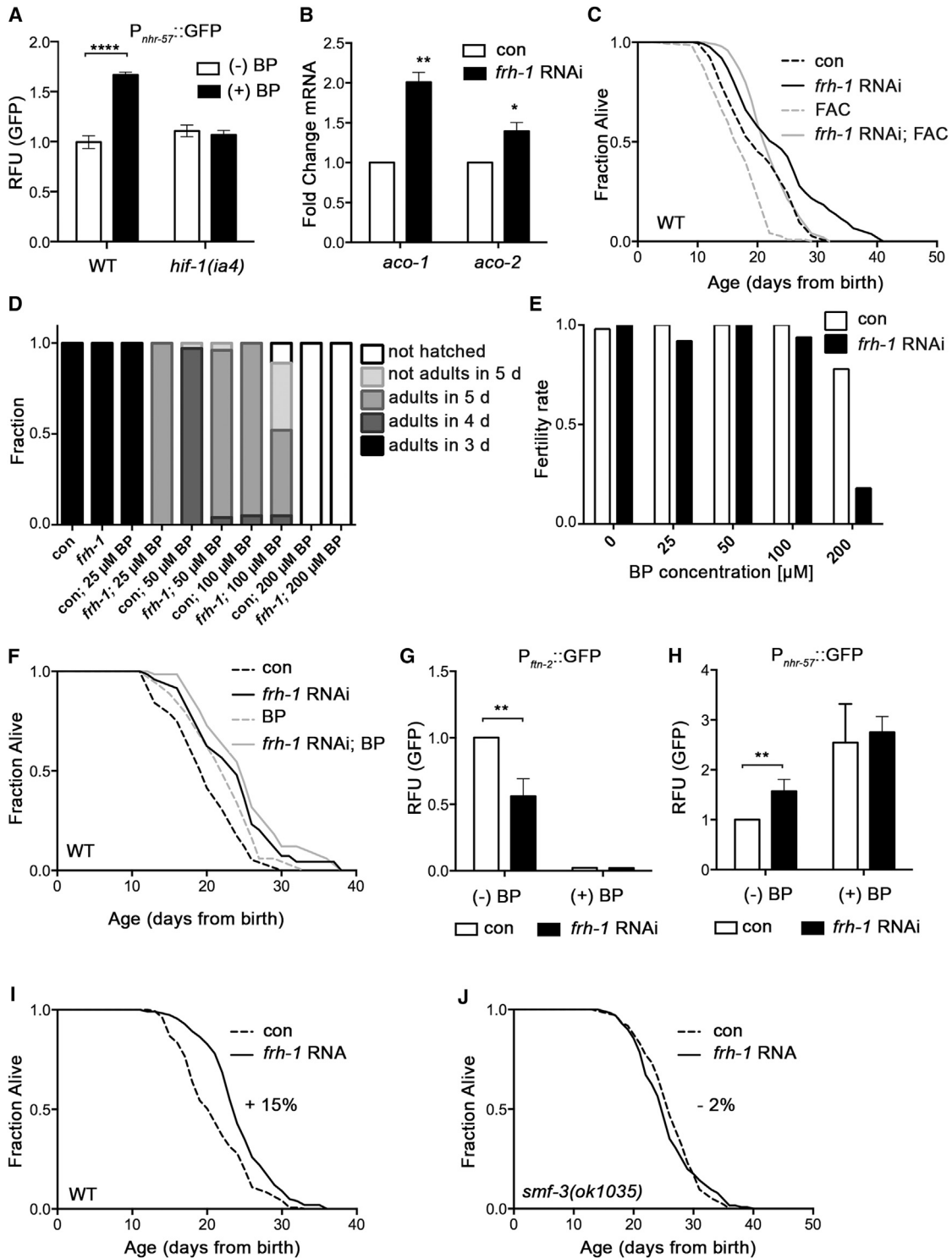


**Figure 4. Frataxin Silencing Extends Lifespan through Iron Deprivation**

(A) Quantification of GFP expression in WT and *hif-1(ia4)* strains expressing the  $P_{nhr-57}::GFP$  transgene, left untreated or treated for 24 hr with 100  $\mu$ M of the iron chelator 2,2'-dipyridyl (BP), is shown.

(B) Quantification of *aconitases* transcript expression in WT animals fed bacteria transformed with either empty-vector (con) or vector-expressing dsRNA against *frh-1* (*frh-1* RNAi) is shown.

(C) Kaplan-Meier survival curves of WT animals fed as in (B) and left untreated or treated from eggs with life-shortening concentration (6.6 mg/ml) of an iron donor [ammonium iron (III) citrate, FAC] are shown.

(D) Developmental rate of WT animals fed as in (B), and left untreated or treated from eggs with the indicated concentrations of BP, is shown.

(legend continued on next page)



mitophagy (Figure 5A). Depletion of mitophagy regulatory genes significantly prevented this effect (Figure 5A) and also partially suppressed lifespan extension in response to iron depletion (Figures 5B–5E; Table S1). Notably, frataxin silencing did not further increase the effects of iron chelation on the accumulation of the autophagosomes and mitophagy (Figures 5F and 5G). This correlates with the lack of cumulative effect of the two treatments on lifespan (Figure 4F), and it suggests mitochondrial degradation by the lysosomal pathway as a specific mechanism induced by frataxin suppression to extend lifespan via cytosolic iron deprivation.

Whereas mitochondrial stress and iron deprivation converge on mitophagy to extend lifespan, the different phenotypic appearances of long-lived iron-depleted and frataxin-deficient animals (Figure 6A) also suggest the induction of incompletely overlapping signaling between the two treatments. While 4-day-old frataxin-depleted animals displayed their typical reduced size and fecundity compared to control animals, life-extending doses of iron chelation affected neither animal size nor fecundity (Figure 6A). The iron chelator reduced fecundity to the same level of *frh-1* RNAi only at doses of 100  $\mu$ M (Figure S4G), which also dramatically impaired animal development (Figure 4D). As a first indication that frataxin and iron depletion can also act through non-overlapping mechanisms, while *frh-1* RNAi did not extend lifespan of the *hif-1* mutants (Figure 3C), iron chelation could still do so (although the two treatments were not fully additive) (Figures 6B and 6C).

We then looked at *hif-1* upstream and downstream regulatory genes. The absence of EGL-9, the *C. elegans* homolog of the HIF-1 prolyl-hydroxylase, stabilizes *hif-1* in normoxia conditions and extends lifespan [9]. As expected by the fact that the prolyl-hydroxylase can be inhibited by low iron content [10], iron chelation did not extend lifespan of the long-lived *egl-9* mutants (Figures 6D and 6E). However, contrary to our expectation, *frh-1* RNAi not only further extended lifespan of the long-lived *egl-9* mutants but it also significantly suppressed animals internal bagging due to the egg-laying defect described in this strain (Figures 6D and 6E; Table S1). We then confirmed the induction of some globin genes (*glb-10*, *glb-19*, and *glb-28*) and the reduction of *glb-26* upon *frh-1* RNAi by quantifying the expression of the corresponding GFP reporter strains through an unbiased automated microscopy platform (Figure 6F). Iron chelation also upregulated *glb-10* expression and this was not further increased by *frh-1* RNAi (Figure 6G). However, surprisingly, loss of *glb-10* suppressed *frh-1* RNAi longevity, but did not prevent the pro-longevity effect of the iron chelator (Figures 6H, 6I, S5A, and S5B; Table S1). Taken together, our data reveal that overlapping (mitophagy) as well as unique (*egl-9* and *glb-10*) hypoxia-related pathways specify longevity of frataxin- and iron-depleted animals.

## DISCUSSION

Collectively, our findings indicate that an iron starvation, hypoxia-like response is triggered by frataxin silencing and activates an evolutionarily conserved *pdr-1*/Parkin- and *dct-1*/Bnip3-regulated mitophagy, which ultimately mediates lifespan extension in *C. elegans*. To our knowledge, this is the first study that addressed and clearly identified a causal role for mitochondrial autophagy in longevity specification. ROS-dependent activation of HIF-1 is required for the lifespan extension of genetic-derived *Mit* mutants [28]. However, ROS are not deemed to be the main longevity determinants of RNAi-derived *Mit* mutants [7, 43], and induction of mitophagy can reduce ROS levels in response to hypoxia [13]. Consistent with these observations, we found that silencing of different MRC regulatory genes reduces ROS content. Although it is still possible that a transient elevation of ROS during animal development activates *hif-1*, our findings are in agreement with the notion that genetic- and RNAi-mediated *Mit* mutants can elicit distinct pro-longevity responses [44]. In fact, our study identifies reduced cytosolic iron, rather than increased ROS levels, as a trigger of the pro-longevity response induced by frataxin silencing. Accordingly, iron is active in the generation of ROS via the Fenton reaction, and, therefore, its reduced cytosolic content may concur to the observed reduced ROS levels in the different RNAi-mediated *Mit* mutants.

Iron is an essential element involved in the biogenesis and activity of different proteins and enzymes, and alteration in iron homeostasis is often observed in mitochondrial-associated disorders. Severe iron deficiency leads in humans to different diseases often associated with developmental defects, and in *C. elegans* it leads to a developmental arrest, which also is seen in response to severe hypoxia or mitochondrial stress. Interestingly, as with mild hypoxia or mitochondrial stress, we found that moderate iron depletion can also have beneficial, pro-longevity effects. This adaptive response, coupled with the resistance to hypoxia observed in the *Mit* mutants ([45] and data not shown), resembles the evolutionarily conserved beneficial effects elicited by hypoxia preconditioning [46]. In neurons and cardiomyocytes, this can be ascribed to activation of autophagy [47], thus suggesting that mitochondrial autophagy could also specifically contribute to its protective effect. Our findings are, therefore, extremely relevant in light of (1) the growing body of evidence implicating altered mitophagy in the pathogenesis of different genetic or age-related (neuro)degenerative disorders [15, 16], and (2) the beneficial effects that could be provided by the hypoxia mimetic effect of iron chelators in these pathological conditions.

In support of mitophagy being induced as part of the protective iron starvation response activated to cope with mitochondrial

(E) Number of eggs hatched per worm was quantified and normalized against the number of eggs laid (fertility rate) in WT animals fed bacteria transformed as in (B), after L4 larvae were left untreated or treated for 24 hr with the indicated concentrations of BP.

(F) Kaplan-Meier survival analysis of WT animals fed bacteria transformed with either empty-vector (con) or vector-expressing dsRNA against *frh-1* (*frh-1* RNAi), and left untreated or treated from eggs with 10  $\mu$ M BP, is shown.

(G) Automated fluorescent quantification of GFP expression in *P<sub>frh-2</sub>::GFP* transgenic strain fed as in (F), and left untreated or treated for 18 hr as L4 with 100  $\mu$ M BP, is shown.

(H) Automated fluorescent quantification of GFP expression in *P<sub>frh-57</sub>::GFP* transgenic strain treated as in (G) is shown.

(I and J) Kaplan-Meier survival analysis of WT animals and *smf-3(ok1035)* mutants fed as in (B).

Bar graph represents means  $\pm$  SEM (n = 3); \*p value versus con < 0.05, \*\*p value versus con < 0.01, \*\*\*\*p value versus con < 0.0001. See also Figure S4D.

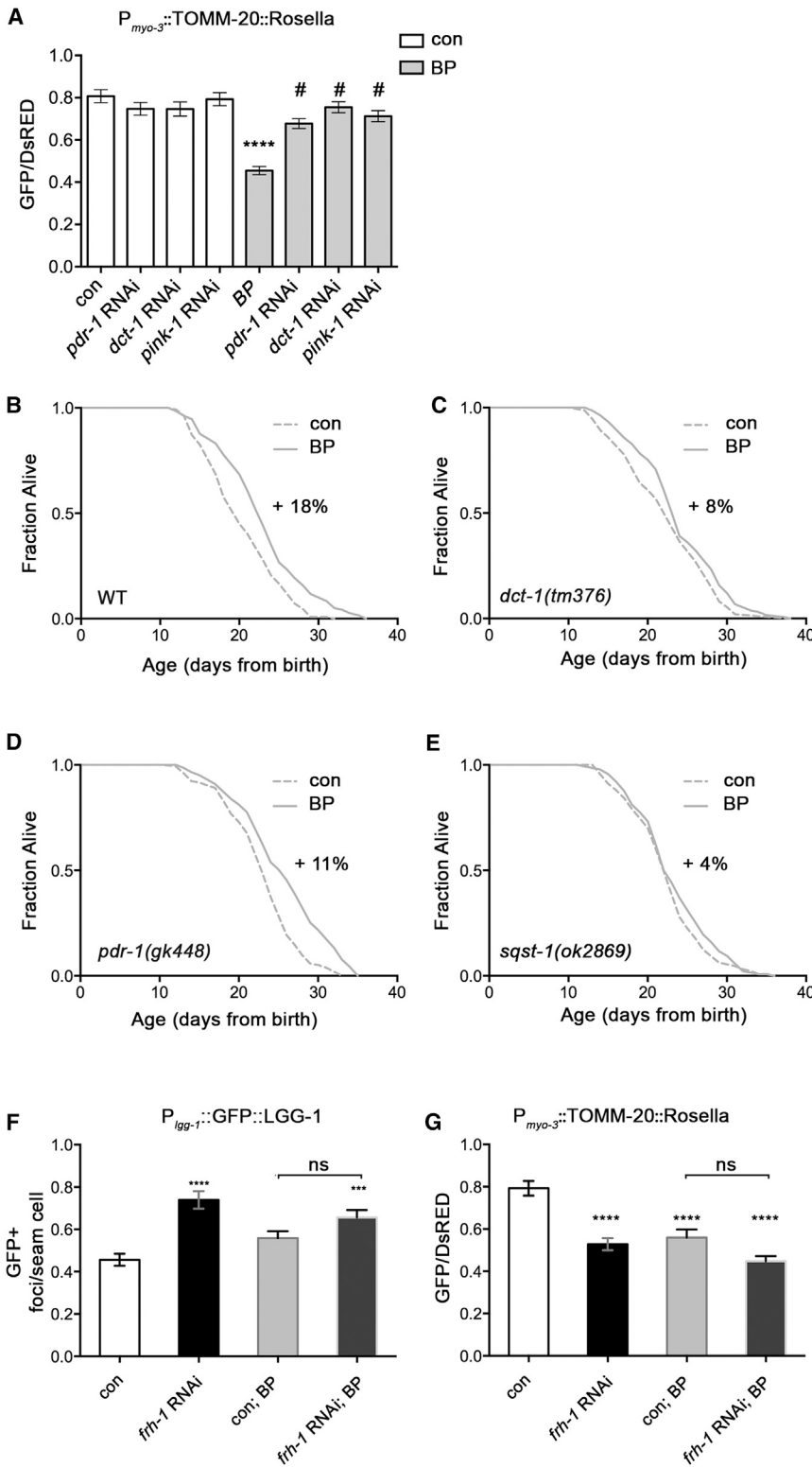


**Figure 5. Iron Deprivation Extends Lifespan through the Induction of Mitophagy**

(A) Quantification of the ratio between GFP/DsRED in  $P_{myo-3}::TOMM-20::Rosella$  transgenic animals fed bacteria transformed with either empty vector (con) or vector expressing the indicated dsRNA, and left untreated or treated from eggs with 10  $\mu$ M of the iron chelator BP, is shown.

(B–E) Kaplan-Meier survival curves of WT animals, *dct-1(tm376)*, *pdr-1(gk448)*, and *sqst-1(ok2869)* strains, left untreated or treated from eggs with 10  $\mu$ M BP, are shown.

(F and G) Quantifications of GFP+ foci in the seam cells and of the ratio between GFP/DsRED, respectively, in  $P_{igg-1}::GFP::LGG-1$  (F) and in  $P_{myo-3}::TOMM-20::Rosella$  (G) transgenic strains fed bacteria transformed with empty-vector (con) or with vector-expressing dsRNA against *frh-1* (*frh-1* RNAi), and left untreated or treated from eggs with 10  $\mu$ M of BP, are shown.

Bar graphs represent means  $\pm$  SEM (n = 5); \*\*\*p value versus con < 0.001, \*\*\*\*p value versus con < 0.0001, #p value versus *frh-1* RNAi < 0.0001; NS, non-significant.

prisingly, while mutants or silencing of different mitophagy regulatory genes, namely *pdr-1*, *dct-1*, and *sqst-1*, as well as silencing of *pink-1*, in part or completely suppressed lifespan extension upon frataxin suppression, two different *pink-1* alleles did not. These findings are consistent with those of Bess et al. [19] showing that *pink-1* mutants do not exacerbate the developmental arrest elicited by UVC-induced mtDNA damage, while *pink-1* silencing prevents proper elimination of damaged mtDNA after UVC irradiation and suggests that *pink-1* mutants may retain some residual functions required for animal somatic maintenance (development or longevity) in response to mitochondrial stress. Taken together, we revealed a conserved function for mitophagy regulatory genes in mitochondrial elimination in *C. elegans*, and we identified a novel protective role for mitophagy in longevity specification in response to mitochondrial stress and iron deprivation.

Interestingly, while we were working on this paper, it was shown that iron chelators can induce mitophagy in mammalian cells [48] and in *C. elegans* [49], possibly as a way of recycling iron from the mitochondrial storage. These findings insinuate that, although frataxin silencing

stress, we show that different mitophagy regulatory genes mediate mitophagy induction and lifespan extension upon frataxin or iron depletion, and that the effect of the two combined treatments on mitophagy and on lifespan is not additive. Sur-

can induce mitophagy via cytosolic iron deprivation, the non-additive effects of the two combined treatments could also be a consequence of iron depletion-induced mitochondrial damage. It will be important to further elucidate underlying molecular

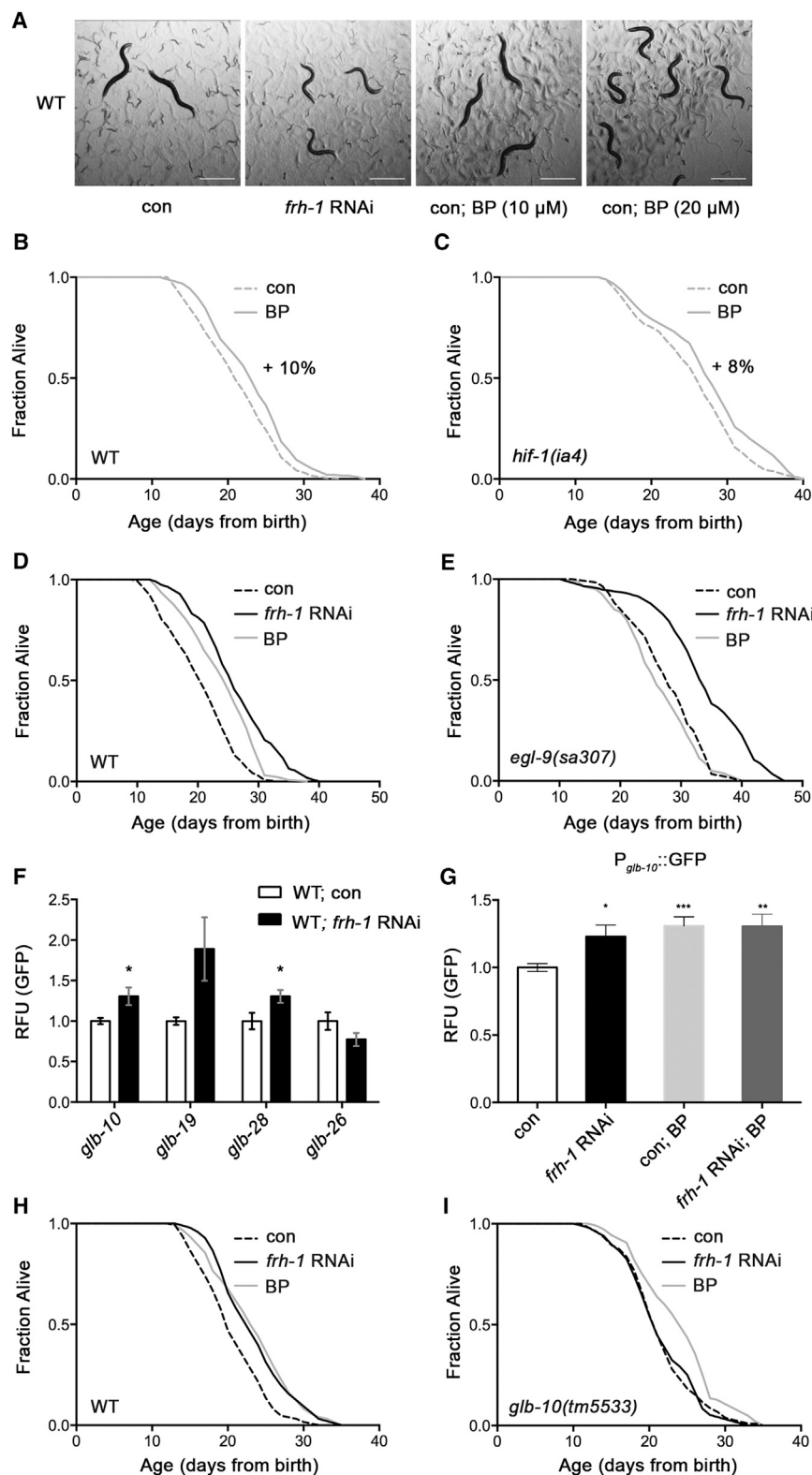


**Figure 6. Frataxin and Iron Depletion Act through Independent Pathways**

(A) Representative picture of 4-day-old WT worms fed bacteria transformed with empty-vector (con) or with vector-expressing dsRNA against *frh-1* (*frh-1* RNAi) and fed empty vector expressing bacteria and treated from eggs with the indicated concentrations of the iron chelator BP. Pictures were acquired using 40-fold magnification on a stereomicroscope (Leica MZ10F). White scale bars, 500  $\mu$ m.

(B and C) Kaplan-Meier survival curves of WT (B) and *hif-1(ia4)* (C) strains left untreated or treated from eggs with 10  $\mu$ M of BP are shown.

(D and E) Kaplan-Meier survival curves of WT (D) and *egl-9(sa307)* (E) strain fed bacteria transformed with empty-vector left untreated (con) or treated from eggs with 10  $\mu$ M BP or fed bacteria transformed with vector-expressing dsRNA against *frh-1* (*frh-1* RNAi) are shown.

(F) Automated fluorescent quantification of GFP expression in  $P_{glb-10}::GFP$ ,  $P_{glb-19}::GFP$ ,  $P_{glb-28}::GFP$  and  $P_{glb-26}::GFP$  transgenic strains fed bacteria transformed with empty-vector (con) or with vector-expressing dsRNA against *frh-1* (*frh-1* RNAi). Bars and errors represent means  $\pm$  SEM (n = 3); \*p value versus con < 0.05.

(G) Automated fluorescent quantification of GFP expression in the  $P_{glb-10}::GFP$  transgenic strain fed as in (F) and left untreated or treated from eggs with the iron 10  $\mu$ M BP is shown. Bars and errors represent means  $\pm$  SEM (n = 3); \*p value versus con < 0.05, \*\*p value versus con < 0.01, \*\*\*p value versus con < 0.001.

(H and I) Kaplan-Meier survival curves of WT and *glb-10(tm5533)* strains fed as in (D) and (E). See also Figure S5.

mechanisms of iron- and frataxin-depletion induction of mitophagy and to understand whether mitophagy plays a causal role in health span determination in other pathophysiological conditions.

span. Indeed, although *glb-10* was upregulated also by iron chelation, *glb-10* mutants did not affect their longevity, and *glb-10* overexpression by transgene injection did not positively impact on lifespan in otherwise wild-type animals (data not shown). On

the other hand, contrary to frataxin silencing, the lifespan-extending effect of iron deprivation was still present in the *hif-1* mutants, while it was completely abolished by lack of EGL-9, the prolyl-hydroxylase responsible for HIF-1 degradation in normoxia conditions, suggesting the parallel existence of *hif-1*-independent pathways to modulate iron-depletion extension of lifespan possibly mediated by other *egl-9* substrates. Interestingly, EGL-9 is inhibited by low oxygen levels but also by reduced levels of iron, and it can act in an *hif-1*-dependent or -independent manner [51], while globins can act as oxygen sensing, as NADH oxidase to sustain anaerobic respiration, and as ROS/NOS-scavenging proteins, and their expression can be induced in an *hif-1*-dependent manner [36, 37]. Additional studies to accurately assess tissue-specific expression of the different globins and to investigate possible links between the different *hif-1*-dependent or -independent signaling networks are required to elucidate their role in longevity specification in response to mitochondrial stress and/or iron depletion.

In *C. elegans*, *hif-1* can promote or limit longevity through distinct molecular mechanisms [52], and our data indicate that it can also act as a positive or negative regulator of autophagy. We found that *hif-1* was partially required for frataxin extension of lifespan and induction of autophagy. Given that additional transcription factors, such as p53/CEP-1 or HLH-30, can regulate *Mit* mutants' longevity through autophagy [6, 53], it is attractive to speculate a crosstalk between transcription factors in mediating mitochondrial stress and/or iron-depletion extension of lifespan through autophagy. In line with this possibility, iron chelation and hypoxia modulate the expression of common HIF-1 and p53 targets, including mitophagy in mammals [13, 48], and frataxin participates in the hypoxia-induced response together with the two transcription factors [54]. In conclusion, this is the first study that to our knowledge identifies a causal role for mitophagy as part of a pro-longevity iron starvation response induced to cope with mitochondrial stress, thus opening new interesting possibilities for healthy aging medicine. Since autophagy is implicated in the pathogenesis and treatment of several neurodegenerative disorders, it is time to speculate that the same could hold true also for more dedicated forms of autophagy, such as mitophagy, especially in those neurodegenerative disorders, such as FRDA, or age-related diseases associated with progressive mitochondrial deterioration.

## EXPERIMENTAL PROCEDURES

### Mammalian Cells

#### Transfection and Protein Expression Analysis

HEK293 cells were transiently transfected with expression plasmids Sh-scramble and Sh-Frataxin using TurboFect Transfection Reagent (Thermo Scientific), and the expression of the indicated proteins was analyzed by western blot in total cell extracts or mitochondrial fractions or by immunofluorescence analysis. See the [Supplemental Experimental Procedures](#) for details.

### C. elegans

#### Nematode Strains and Culture Conditions

Standard conditions for *C. elegans* strains culture and RNAi experiments were used. All experiments were performed at 20°C on nematode growth media (NGMs) agar supplemented with *Escherichia coli* (OP50 or transformed HT115), unless otherwise indicated. A list of strains utilized in this work is provided in the [Supplemental Experimental Procedures](#).

### Lifespan and Statistical Analysis

Survival analysis started from hatching using synchronous populations of 70–100 animals per strain. Survival curves and statistical analyses were carried out following standard procedures in the *C. elegans* aging field [55]. Briefly, we calculated mean, SD of the mean, and p value using the log-rank test (Mantel-Cox) from Kaplan-Meier survival analysis of pooled data resulting from at least two independent replicas. See the [Supplemental Experimental Procedures](#) for the detailed procedure and [Table S1](#) for the summary of lifespan data analysis.

### Quantification of Gene Expression

GFP expression was quantified either by acquiring pictures with a Imager2 Zeiss fluorescence microscope, followed by ImageJ analysis, or through automated quantification, by transferring transgenic adult-stage worms to 96-well plates followed by image acquisition and analysis with the ArrayScan V<sup>TI</sup> HCS Reader (Cellomics, Thermo Fisher Scientific) [56]. The qRT-PCR was carried out as we previously described. See the [Supplemental Experimental Procedures](#) for detailed quantification methods and analysis.

### Electron Microscopy

Synchronized populations of about ~1,000 first-day adult animals were mixed with a thick pellet of *Escherichia coli* and immediately flash frozen. Thin sections of osmium tetroxide-fixed samples were stained with 2% uranyl acetate and Reynold's lead citrate and imaged at 80 kV on a Phillips CM10 electron microscope. Representative images were acquired from two experiments. None of the wild-type animals displayed dark electron-dense granules, while all sections from *frh-1* RNAi animals displayed dark deposits in at least one mitochondrion. See the [Supplemental Experimental Procedures](#) for more details.

### Iron Chelation Sensitivity

The iron chelator 2,2'-dipyridyl (BP, Carl Roth) was supplemented to NGM at the indicated concentrations, and its effect was investigated on development, fecundity, and fertility of synchronized populations of worms. Transgene expression in response to iron chelation was measured on synchronized larvae grown for 24 hr on NGM plates and then transferred as L4 larvae to NGM plates supplemented with 100 μM BP for 18 hr before quantification.

### Hypoxia Treatment

For generation of hypoxic status, worms were placed into a modular incubator chamber (Billups-Rothenberg). For almost complete replacement of the oxygen (<0.1%), a gas mixture (95% N<sub>2</sub>, 5% CO<sub>2</sub>) was flushed (15 l/min) into the chamber for 10 min. Young adult worms were then left in the hypoxic chamber for 4 hr at 20°C. Immediately after the hypoxia treatment, the worms were placed on a slide and acquired with the respective control left untreated.

### Autophagy Measurements

Different transgenic strains were used to quantify autophagosomes using 100-fold magnification on a Zeiss Axio Imager 2 microscope. GFP-positive foci were counted in the seam cells of *gfp::lgg-1* L3 larvae and in the anterior pharyngeal bulb of young adult *sqst-1::gfp* animals. mCherry/*lgg-1*-positive foci were counted in the intestine of young adult worms. See the [Supplemental Experimental Procedures](#) for the detailed procedure.

### Mitophagy Measurement

For monitoring of mitophagy, the following four newly generated *C. elegans* transgenic strains were employed: (1) N2;*s*[*p<sub>myo-3</sub>::mtGFP*];*Ex*[*p<sub>lgg-1</sub>::DsRed::LGG-1*], (2) N2;*Ex*[*p<sub>myo-3</sub>::PDR-1::DsRed*; *p<sub>dct-1</sub>::DCT-1::GFP*], (3) N2;*Ex*[*p<sub>myo-3</sub>::DsRed::LGG-1*; *p<sub>dct-1</sub>::DCT-1::GFP*], and (4) N2;*Ex*[*p<sub>myo-3</sub>::TOMM-20::Rosella*]. See the [Supplemental Experimental Procedures](#) for details.

### Mitochondrial Density

Mitochondrial density, expressed as the percentage of mitochondrial volume in the total analyzed volume, was quantified through 3D reconstruction of z stack images acquired using confocal laser scanning microscopy from *rps-0p::gas-1::DENDRA2* transgenic strain, as previously described. See the [Supplemental Experimental Procedures](#) for details.

### Statistical Analysis

Data are represented as mean ± SEM from at least three independent biological replica carried out with blinded genotypes where possible. Statistical analyses were performed using two-tailed Student's t test or one-way ANOVA for multiple comparisons (GraphPad software) to calculate significance as follows: \*p = 0.01 to 0.05, \*\*p = 0.001 to 0.01, \*\*\*p = 0.0001 to 0.001, and \*\*\*\*p < 0.0001 versus respective control conditions.



## SUPPLEMENTAL INFORMATION

Supplemental Information includes Supplemental Experimental Procedures, five figures, and one table and can be found with this article online at <http://dx.doi.org/10.1016/j.cub.2015.05.059>.

## AUTHOR CONTRIBUTIONS

Conceptualization, N.V.; Methodology, A. Schiavi, S.M., K.P.; Investigation, A. Schiavi, S.M., A. Shaik, K.P., F.S., V.B., A.T., N.C., S.D.H., N.V.; Formal Analysis, A. Schiavi, N.V.; Writing – Original Draft, N.V., A. Schiavi; Writing – Review & Editing, N.V., A. Schiavi, A.T., B.P.B., N.T.; Resources, N.V., B.P.B., F.C., N.T.; Funding Acquisition and Supervision, N.V.

## ACKNOWLEDGMENTS

Most nematode strains utilized in this work were provided by the *Caenorhabditis* Genetics Center, funded by the NIH Office of Research Infrastructure Programs (P40 OD010440). Other strains were kindly provided by Jo Anne Powell-Coffman (ZG120 and ZG175), Chris Link (VC1024 and RB2547), and Joshua Romney (XA6901). We thank Virginia Fonte for critical reading of the manuscript and technical help with electron microscopy, Anthea Di Rita and Beatrice Biferali for technical assistance with experiments in mammalian cells, and Roberto Testi for Sh-Frataxin and control plasmids. B.P.B. is indebted to the Fund for Scientific Research – Flanders (G008912N). This work was financially supported by funding to N.V. from the following: Italian Association for Cancer Research (MFA11509), Strategic Research Funding of the Heinrich Heine University (701301988), and Start-up Competitive Research Funding of the Medical Faculty of the Heinrich Heine University (Forschungskommision 43/2013).

Received: January 28, 2015

Revised: May 4, 2015

Accepted: May 27, 2015

Published: July 2, 2015

## REFERENCES

- Campuzano, V., Montermini, L., Moltò, M.D., Pianese, L., Cossée, M., Cavalcanti, F., Monros, E., Rodius, F., Duclos, F., Monticelli, A., et al. (1996). Friedreich's ataxia: autosomal recessive disease caused by an intronic GAA triplet repeat expansion. *Science* *271*, 1423–1427.
- Ventura, N., and Rea, S.L. (2007). *Caenorhabditis elegans* mitochondrial mutants as an investigative tool to study human neurodegenerative diseases associated with mitochondrial dysfunction. *Biotechnol. J.* *2*, 584–595.
- Dell'agnello, C., Leo, S., Agostino, A., Szabadkai, G., Tiveron, C., Zulian, A., Prella, A., Roubertoux, P., Rizzuto, R., and Zeviani, M. (2007). Increased longevity and refractoriness to Ca(2+)-dependent neurodegeneration in Surf1 knockout mice. *Hum. Mol. Genet.* *16*, 431–444.
- Ventura, N., Rea, S.L., and Testi, R. (2006). Long-lived *C. elegans* mitochondrial mutants as a model for human mitochondrial-associated diseases. *Exp. Gerontol.* *41*, 974–991.
- Munkácsy, E., and Rea, S.L. (2014). The paradox of mitochondrial dysfunction and extended longevity. *Exp. Gerontol.* *56*, 221–233.
- Schiavi, A., Torgovnick, A., Kell, A., Megalou, E., Castelein, N., Guccini, I., Marzocchella, L., Gelino, S., Hansen, M., Malisan, F., et al. (2013). Autophagy induction extends lifespan and reduces lipid content in response to frataxin silencing in *C. elegans*. *Exp. Gerontol.* *48*, 191–201.
- Durieux, J., Wolff, S., and Dillin, A. (2011). The cell-non-autonomous nature of electron transport chain-mediated longevity. *Cell* *144*, 79–91.
- Mehta, R., Steinkraus, K.A., Sutphin, G.L., Ramos, F.J., Shamieh, L.S., Huh, A., Davis, C., Chandler-Brown, D., and Kaerberlein, M. (2009). Proteasomal regulation of the hypoxic response modulates aging in *C. elegans*. *Science* *324*, 1196–1198.
- Zhang, Y., Shao, Z., Zhai, Z., Shen, C., and Powell-Coffman, J.A. (2009). The HIF-1 hypoxia-inducible factor modulates lifespan in *C. elegans*. *PLoS ONE* *4*, e6348.
- Epstein, A.C., Gleadle, J.M., McNeill, L.A., Hewitson, K.S., O'Rourke, J., Mole, D.R., Mukherji, M., Metzen, E., Wilson, M.I., Dhanda, A., et al. (2001). *C. elegans* EGL-9 and mammalian homologs define a family of dioxygenases that regulate HIF by prolyl hydroxylation. *Cell* *107*, 43–54.
- Samokhvalov, V., Scott, B.A., and Crowder, C.M. (2008). Autophagy protects against hypoxic injury in *C. elegans*. *Autophagy* *4*, 1034–1041.
- Wang, K., and Klionsky, D.J. (2011). Mitochondria removal by autophagy. *Autophagy* *7*, 297–300.
- Zhang, H., Bosch-Marce, M., Shimoda, L.A., Tan, Y.S., Baek, J.H., Wesley, J.B., Gonzalez, F.J., and Semenza, G.L. (2008). Mitochondrial autophagy is an HIF-1-dependent adaptive metabolic response to hypoxia. *J. Biol. Chem.* *283*, 10892–10903.
- Schiavi, A., and Ventura, N. (2014). The interplay between mitochondria and autophagy and its role in the aging process. *Exp. Gerontol.* *56*, 147–153.
- Palikaras, K., and Tavernarakis, N. (2012). Mitophagy in neurodegeneration and aging. *Front. Genet.* *3*, 297.
- Narendra, D.P., and Youle, R.J. (2011). Targeting mitochondrial dysfunction: role for PINK1 and Parkin in mitochondrial quality control. *Antioxid. Redox Signal.* *14*, 1929–1938.
- Springer, W., Hoppe, T., Schmidt, E., and Baumeister, R. (2005). A *Caenorhabditis elegans* Parkin mutant with altered solubility couples alpha-synuclein aggregation to proteotoxic stress. *Hum. Mol. Genet.* *14*, 3407–3423.
- Sämann, J., Hegermann, J., von Gromoff, E., Eimer, S., Baumeister, R., and Schmidt, E. (2009). *Caenorhabditis elegans* LRK-1 and PINK-1 act antagonistically in stress response and neurite outgrowth. *J. Biol. Chem.* *284*, 16482–16491.
- Bess, A.S., Crocker, T.L., Ryde, I.T., and Meyer, J.N. (2012). Mitochondrial dynamics and autophagy aid in removal of persistent mitochondrial DNA damage in *Caenorhabditis elegans*. *Nucleic Acids Res.* *40*, 7916–7931.
- Yasuda, M., D'Sa-Eipper, C., Gong, X.L., and Chinnadurai, G. (1998). Regulation of apoptosis by a *Caenorhabditis elegans* BNIP3 homolog. *Oncogene* *17*, 2525–2530.
- Tian, Y., Li, Z., Hu, W., Ren, H., Tian, E., Zhao, Y., Lu, Q., Huang, X., Yang, P., Li, X., et al. (2010). *C. elegans* screen identifies autophagy genes specific to multicellular organisms. *Cell* *141*, 1042–1055.
- Pursiheimo, J.P., Rantanen, K., Heikkinen, P.T., Johansen, T., and Jaakkola, P.M. (2009). Hypoxia-activated autophagy accelerates degradation of SQSTM1/p62. *Oncogene* *28*, 334–344.
- Guo, B., Huang, X., Zhang, P., Qi, L., Liang, Q., Zhang, X., Huang, J., Fang, B., Hou, W., Han, J., and Zhang, H. (2014). Genome-wide screen identifies signaling pathways that regulate autophagy during *Caenorhabditis elegans* development. *EMBO Rep.* *15*, 705–713.
- Okatsu, K., Saisho, K., Shimanuki, M., Nakada, K., Shitara, H., Sou, Y.S., Kimura, M., Sato, S., Hattori, N., Komatsu, M., et al. (2010). p62/SQSTM1 cooperates with Parkin for perinuclear clustering of depolarized mitochondria. *Genes Cells* *15*, 887–900.
- Palikaras, K., and Tavernarakis, N. (2014). Mitochondrial homeostasis: the interplay between mitophagy and mitochondrial biogenesis. *Exp. Gerontol.* *56*, 182–188.
- Huang, M.L., Becker, E.M., Whitnall, M., Suryo Rahmanto, Y., Ponka, P., and Richardson, D.R. (2009). Elucidation of the mechanism of mitochondrial iron loading in Friedreich's ataxia by analysis of a mouse mutant. *Proc. Natl. Acad. Sci. USA* *106*, 16381–16386.
- Kirienko, N.V., Kirienko, D.R., Larkins-Ford, J., Wählby, C., Ruvkun, G., and Ausubel, F.M. (2013). *Pseudomonas aeruginosa* disrupts *Caenorhabditis elegans* iron homeostasis, causing a hypoxic response and death. *Cell Host Microbe* *13*, 406–416.

28. Lee, S.J., Hwang, A.B., and Kenyon, C. (2010). Inhibition of respiration extends *C. elegans* life span via reactive oxygen species that increase HIF-1 activity. *Curr. Biol.* *20*, 2131–2136.
29. Bellot, G., Garcia-Medina, R., Gounon, P., Chiche, J., Roux, D., Pouyssegur, J., and Mazure, N.M. (2009). Hypoxia-induced autophagy is mediated through hypoxia-inducible factor induction of BNIP3 and BNIP3L via their BH3 domains. *Mol. Cell. Biol.* *29*, 2570–2581.
30. Papandreou, I., Lim, A.L., Laderoute, K., and Denko, N.C. (2008). Hypoxia signals autophagy in tumor cells via AMPK activity, independent of HIF-1, BNIP3, and BNIP3L. *Cell Death Differ.* *15*, 1572–1581.
31. Dillin, A., Hsu, A.L., Arantes-Oliveira, N., Lehrer-Graiwer, J., Hsin, H., Fraser, A.G., Kamath, R.S., Ahringer, J., and Kenyon, C. (2002). Rates of behavior and aging specified by mitochondrial function during development. *Science* *298*, 2398–2401.
32. Khan, M.H., Ligon, M., Hussey, L.R., Hufnal, B., Farber, R., 2nd, Munkacsy, E., Rodriguez, A., Dillow, A., Kahlig, E., and Rea, S.L. (2013). TAF-4 is required for the life extension of *isp-1*, *clk-1* and *tpk-1* Mit mutants. *Aging (Albany NY)* *5*, 741–758.
33. Meléndez, A., Tallóczy, Z., Seaman, M., Eskelinen, E.L., Hall, D.H., and Levine, B. (2003). Autophagy genes are essential for dauer development and life-span extension in *C. elegans*. *Science* *301*, 1387–1391.
34. Jiang, H., Guo, R., and Powell-Coffman, J.A. (2001). The *Caenorhabditis elegans* *hif-1* gene encodes a bHLH-PAS protein that is required for adaptation to hypoxia. *Proc. Natl. Acad. Sci. USA* *98*, 7916–7921.
35. Shen, C., Nettleton, D., Jiang, M., Kim, S.K., and Powell-Coffman, J.A. (2005). Roles of the HIF-1 hypoxia-inducible factor during hypoxia response in *Caenorhabditis elegans*. *J. Biol. Chem.* *280*, 20580–20588.
36. Hoogewijs, D., Terwilliger, N.B., Webster, K.A., Powell-Coffman, J.A., Tokishita, S., Yamagata, H., Hankeln, T., Burmester, T., Rytönen, K.T., Nikinmaa, M., et al. (2007). From critters to cancers: bridging comparative and clinical research on oxygen sensing, HIF signaling, and adaptations towards hypoxia. *Integr. Comp. Biol.* *47*, 552–577.
37. Hoogewijs, D., Geuens, E., Dewilde, S., Vierstraete, A., Moens, L., Vinogradov, S., and Vanfleteren, J.R. (2007). Wide diversity in structure and expression profiles among members of the *Caenorhabditis elegans* globin protein family. *BMC Genomics* *8*, 356.
38. Romney, S.J., Newman, B.S., Thacker, C., and Leibold, E.A. (2011). HIF-1 regulates iron homeostasis in *Caenorhabditis elegans* by activation and inhibition of genes involved in iron uptake and storage. *PLoS Genet.* *7*, e1002394.
39. Gabrielli, N., Ayté, J., and Hidalgo, E. (2012). Cells lacking *pfh1*, a fission yeast homolog of mammalian frataxin protein, display constitutive activation of the iron starvation response. *J. Biol. Chem.* *287*, 43042–43051.
40. Kim, Y.I., Cho, J.H., Yoo, O.J., and Ahnn, J. (2004). Transcriptional regulation and life-span modulation of cytosolic aconitase and ferritin genes in *C. elegans*. *J. Mol. Biol.* *342*, 421–433.
41. Gourley, B.L., Parker, S.B., Jones, B.J., Zumbrennen, K.B., and Leibold, E.A. (2003). Cytosolic aconitase and ferritin are regulated by iron in *Caenorhabditis elegans*. *J. Biol. Chem.* *278*, 3227–3234.
42. Puccio, H., Simon, D., Cossée, M., Criqui-Filipe, P., Tiziano, F., Melki, J., Hindelang, C., Matyas, R., Rustin, P., and Koenig, M. (2001). Mouse models for Friedreich ataxia exhibit cardiomyopathy, sensory nerve defect and Fe-S enzyme deficiency followed by intramitochondrial iron deposits. *Nat. Genet.* *27*, 181–186.
43. Rea, S.L., Ventura, N., and Johnson, T.E. (2007). Relationship between mitochondrial electron transport chain dysfunction, development, and life extension in *Caenorhabditis elegans*. *PLoS Biol.* *5*, e259.
44. Yang, W., and Hekimi, S. (2010). Two modes of mitochondrial dysfunction lead independently to lifespan extension in *Caenorhabditis elegans*. *Aging Cell* *9*, 433–447.
45. Butler, J.A., Ventura, N., Johnson, T.E., and Rea, S.L. (2010). Long-lived mitochondrial (Mit) mutants of *Caenorhabditis elegans* utilize a novel metabolism. *FASEB J.* *24*, 4977–4988.
46. Dasgupta, N., Patel, A.M., Scott, B.A., and Crowder, C.M. (2007). Hypoxic preconditioning requires the apoptosis protein CED-4 in *C. elegans*. *Curr. Biol.* *17*, 1954–1959.
47. Park, H.K., Chu, K., Jung, K.H., Lee, S.T., Bahn, J.J., Kim, M., Lee, S.K., and Roh, J.K. (2009). Autophagy is involved in the ischemic preconditioning. *Neurosci. Lett.* *451*, 16–19.
48. Allen, G.F., Toth, R., James, J., and Ganley, I.G. (2013). Loss of iron triggers PINK1/Parkin-independent mitophagy. *EMBO Rep.* *14*, 1127–1135.
49. Kirienko, N.V., Ausubel, F.M., and Ruvkun, G. (2015). Mitophagy confers resistance to siderophore-mediated killing by *Pseudomonas aeruginosa*. *Proc. Natl. Acad. Sci. USA* *112*, 1821–1826.
50. Maglioni, S., Schiavi, A., Runci, A., Shaik, A., and Ventura, N. (2014). Mitochondrial stress extends lifespan in *C. elegans* through neuronal homeostasis. *Exp. Gerontol.* *56*, 89–98.
51. Luhachack, L.G., Visvikis, O., Wollenberg, A.C., Lacy-Hulbert, A., Stuart, L.M., and Irazoqui, J.E. (2012). EGL-9 controls *C. elegans* host defense specificity through prolyl hydroxylation-dependent and -independent HIF-1 pathways. *PLoS Pathog.* *8*, e1002798.
52. Leiser, S.F., and Kaerberlein, M. (2010). The hypoxia-inducible factor HIF-1 functions as both a positive and negative modulator of aging. *Biol. Chem.* *391*, 1131–1137.
53. Lapiere, L.R., De Magalhaes Filho, C.D., McQuary, P.R., Chu, C.C., Visvikis, O., Chang, J.T., Gelino, S., Ong, B., Davis, A.E., Irazoqui, J.E., et al. (2013). The TFEB orthologue HLH-30 regulates autophagy and modulates longevity in *Caenorhabditis elegans*. *Nat. Commun.* *4*, 2267.
54. Guccini, I., Serio, D., Condò, I., Rufini, A., Tomassini, B., Mangiola, A., Maira, G., Anile, C., Fina, D., Pallone, F., et al. (2011). Frataxin participates to the hypoxia-induced response in tumors. *Cell Death Dis.* *2*, e123.
55. Ventura, N., Rea, S.L., Schiavi, A., Torgovnick, A., Testi, R., and Johnson, T.E. (2009). p53/CEP-1 increases or decreases lifespan, depending on level of mitochondrial bioenergetic stress. *Aging Cell* *8*, 380–393.
56. Maglioni, S., Arsalan, N., Franchi, L., Hurd, A., Oipari, A.W., Glick, G.D., and Ventura, N. (2015). An automated phenotype-based microscopy screen to identify pro-longevity interventions acting through mitochondria in *C. elegans*. *Biochim Biophys Acta*. Published online May 12, 2015. <http://dx.doi.org/10.1016/j.bbabi.2015.05.004>.